Protocol-Based Load Frequency Control for Power Systems With Nonhomogeneous Sojourn Probabilities

Jun Cheng, Jiangming Xu, Ju H. Park, *Senior Member, IEEE*, and Michael V. Basin, *Senior Member, IEEE*

***Abstract*—This article is concentrated on the load frequency control for interconnected multiarea power systems (IMAPSs) with nonhomogeneous sojourn probabilities (NSPs) and cyber-attacks. A generalized framework of NSPs is formulated to describe the dynamic behavior of IMAPSs. To govern variations of sojourn probabilities, a deterministic switching signal is introduced using the average dwell-time technique. Essentially, different from the existing protocols, an improved event-triggered protocol that is relevant to the dynamic quantizer parameter is presented, thereby increasing triggering intervals. Furthermore, both denial-of-service and deception attacks, which obey Bernoulli distributions, are considered during information transmission. By virtue of the Lyapunov theory, the mean-square exponential stability of the considered systems is established. Finally, the effectiveness of the obtained results is verified via a numerical example.**

***Index Terms*—Cyber-attacks, event-triggered protocol (ETP), load frequency control (LFC), nonhomogeneous sojourn probabilities (NSPs).**

I. Introduction

PAST decades have witnessed the rapid development of networked control systems (NCSs) owing to their extensive applications, including multiagent, power, and other systems. Note that power systems, well-known as typical NCSs, have long been considered as an essential infrastructure vital to national security. For protecting power systems subject to sudden changes, frequency control is mostly employed as an efficient technique to maintain the system performance. As a result, load frequency control (LFC) plays an indispensable role in the power system to adjust the frequency to a desired value [1]. Following this trend, many control techniques have been applied to handle single/multi-area LFC power systems [2], [3], [4], [5], [6], [7], including proportional-integral control, predictive-based control, distributed control, disturbance rejection-based control, and other control laws.

In practical applications, interconnected multiarea power systems (IMAPSs) always experience faults or trips, which degrade the system performance. These unexpected variations can be modeled by a Markov process (MP) [8], [9], [10]. However, the residence time of the MP obeys a memoryless exponential distribution, which means that the transition probabilities are time independent. To address this limitation, a sojourn probability-based technique was proposed in [11], which requires fewer probability transition values than the traditional MP approach [12], [13]. Sojourn probabilities are easy to obtain via statistical methods, making this approach easier to implement. As such, the sojourn-probability-based strategy has been studied in [11] and [14]. Nevertheless, the above-mentioned studies are focused on the discrete-time domain, and little attention has been paid to the continuous-time case. Besides, many IMAPSs exhibit time-varying behaviors, and time-invariant sojourn probabilities fail to describe the actual situations. To address this gap, nonhomogeneous sojourn probabilities (NSPs) have been introduced in the discrete-time domain [15], where a deterministic switching signal (DSS) regulates variations of sojourn probabilities using the average dwell-time (ADT) technique. However, little attention has been paid to NSPs in continuous-time switched IMAPSs, where acquiring transition probabilities is challenging. Filling this gap motivates the current study.

Due to openness of communication networks, cyber-attacks may lead to instability of switched IMAPSs. The network security problem has received great attention, as cyber-attacks aim to destroy the integrity and availability of information. Therefore, it is of practical significance to analyze the stability of IMAPSs against cyber-attacks. Generally speaking, network attacks can be divided into two categories: 1) denial of service (DoS) attacks [16] and 2) deception attacks (DAs) [17], [18]. DoS attacks block the communication networks and information packets do not arrive on time. DAs destroy the authenticity and integrity of packets by tampering with their contents. Therefore, the security-based control problem has triggered increasing research interest [19], [20]. Although many previous results considered different kinds of attacks, the stability of switched IMAPSs under hybrid

Manuscript received 8 November 2022; revised 3 March 2023; accepted 4 May 2023. Date of publication 17 May 2023; date of current version 18 August 2023. This work was supported in part by the National Natural Science Foundation of China under Grant 12161011 and Grant 62173100, and in part by the Natural Science Foundation of Guangxi Normal University under Grant 2021JC001. This work of Ju H. Park was supported by the National Research Foundation of Korea (NRF) Grant funded by the Korea Government (Ministry of Science and ICT) under Grant 2019R1A5A8080290. This article was recommended by Associate Editor D. Yue. *(Corresponding authors: Ju H. Park; Michael V. Basin.)*

Jun Cheng and Jiangming Xu are with the School of Mathematics and Statistics, Guangxi Normal University, Guilin 541006, China (e-mail: jcheng@gxnu.edu.cn; jiangmingxumath@163.com).

Ju H. Park is with the Department of Electrical Engineering, Yeungnam University, Gyeongsan 38541, Republic of Korea (e-mail: jessie@ynu.ac.kr).

Michael V. Basin is with the Robotics Institute, Ningbo University of Technology, Ningbo 315211, Zhejiang, China, and also with the School of Physical and Mathematical Sciences, Autonomous University of Nuevo Leon, San Nicolás de los Garza 66455, Mexico (e-mail: mbasin@nbut.edu.cn; mikhail.basin@uanl.edu.mx).

Color versions of one or more figures in this article are available at https://doi.org/10.1109/TSMC.2023.3274141.

Digital Object Identifier 10.1109/TSMC.2023.3274141

cyber-attacks has received little attention, which provides another motivation for this work.

Due to limitation of communications in computation ability, many efficient protocols are constructed to regulate the data transmission, such as sampled data, round-robin, event-triggered, and other ones [21], [22], [23], [24], [25]. Among them, event-triggered protocol (ETP) is most utilized [26]. In the framework of ETP, the transmitted data are discarded unless the preset event-triggering condition is met, which avoids resource wasting. To date, many efficient ETPs have been appeared, including static [1], dynamic [27], memory [27], [28], and distributed ETPs [29], [30]. For example, the deep learning algorithm is used in [31] to explore a suitable threshold triggered by dynamic events. In [32], an improved dynamic ETP is employed to save resources. Although a number of valuable results on ETPs have been reported, as shown in [33] and [34], many network-induced phenomena, including quantization effects, have not yet been considered, which may lead to resource wasting in a certain context. This leaves room for further improvement of ETPs associated with quantization effects. As such, this article presents an improved ETP (IETP) to further reduce the frequency of data transmission by using a dynamic quantization strategy.

Based on the above description, a dynamic quantization-based IETP for IMAPSs with NSPs, improving communication efficiency, is studied in this article. The novel contributions are listed as follows.

1) An improved IETP associated with the dynamic quantizer parameter is proposed to govern the data transmission for switched IMAPSs. Compared with traditional ETPs, the proposed IETP is capable of speeding up the convergence rate while achieving greater triggering intervals.
2) Benefiting from the ADT technique, a generalized framework of NSPs subjected to a DSS is presented, and the switched IMAPS is established. In contrast to transition probabilities, the NSPs are easy to measure.
3) A unified framework of cyber-attacks is formulated by taking DoS attacks and DAs into consideration. Considering the newly designed switched IMAPSs, the mean-square exponential stability is established via the Lyapunov theory. Finally, the feasibility of the proposed method is tested via a numerical example.

The remainder of this study is organized as follows: Section II provides the model formulation, and in Section III, sufficient conditions are presented to ensure mean square exponential stability of the power system. Section IV presents numerical simulations, and finally, Section V summarizes the conclusions.

Notations: $\mathrm{diag}_N\{A_i\} = \mathrm{diag}\{A_1, \ldots, A_N\}$ stands for a block-diagonal matrix; $He\{R\} = R + R^\top$; $\mathrm{col}_N\{\chi_i(t)\} = \mathrm{col}\{\chi_2(t), \ldots, \chi_N(t)\}$, $\mathrm{col}\{\cdots\}$ denotes the column vector of a matrix; $\mathcal{E}\{*\}$ indicates the mathematical expectation; $\|*\|$ refers to the Euclidean vector norm. $|\cdot|$ indicates the absolute value of a scalar; Pr stands for occurrence probability; $\mathbb{R}^n$ represents the n-dimensional Euclidean space; $\mathcal{L}_2$ depicts the linear vector space with the property of square integrable; $P > 0 (P \geq 0)$ means that P is a positive (semi-positive)-definite matrix.

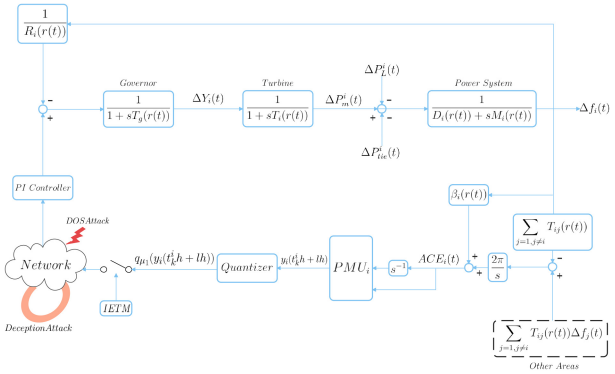

Fig. 1. Diagram of the ith IMAPS with IETP.

II. Problem Statement and Background

In presence of environmental disturbances and component failures, the parameters of power systems are variable, and the variations can be described via an MP. In the sequel, the diagram of the ith IMAPS is depicted in Fig. 1, whose mathematical model can be inferred as follows:

$$\begin{cases} \dot{x}_i(t) = A^{ii}(\vartheta(t))x_i(t) + \sum_{j=1,j\neq i}^{N} A^{ij}(\vartheta(t))x_j(t) \\ \qquad + H^i(\vartheta(t))\Delta P_L^i(t) + B^i(\vartheta(t))u_i(t) \\ y_i(t) = C^i(\vartheta(t))x_i(t) \end{cases} \tag{1}$$

where $x_i(t) \in \mathbb{R}^5$, $y_i(t) \in \mathbb{R}^2$, $u_i(t) \in \mathbb{R}$, and $\Delta P_L^i(t) \in \mathcal{L}_2[0, \infty)$ represent the state, the output, the input, and the load disturbance, respectively, and

$$y_i(t) = \begin{bmatrix} ACE_i & \int_0^t ACE_i(s)ds \end{bmatrix}^\top$$

$$x_i(t) = \begin{bmatrix} \Delta f_i(t) & \Delta P_m^i(t) & \Delta Y_i(t) & \Delta P_{tie}^i(t) & \int_0^t ACE_i(s)ds \end{bmatrix}^\top$$

$$B_i(\vartheta(t)) = \begin{bmatrix} 0 & 0 & \frac{1}{T_g(i)(\vartheta(t))} & 0 & 0 \end{bmatrix}^\top$$

$$H_i(\vartheta(t)) = \begin{bmatrix} -\frac{1}{M_i(\vartheta(t))} & 0 & 0 & 0 & 0 \end{bmatrix}^\top$$

$$C_i(\vartheta(t)) = \begin{bmatrix} \beta_i(\vartheta(t)) & 0 & 0 & 1 & 0 \\ 0 & 0 & 0 & 0 & 1 \end{bmatrix}$$

$$A_{ii}(\vartheta(t)) = \begin{bmatrix} -\frac{D_i(\vartheta(t))}{M_i(\vartheta(t))} & \frac{1}{D_i(\vartheta(t))} & 0 & -\frac{1}{D_i(\vartheta(t))} & 0 \\ 0 & -\frac{1}{T_t^i(\vartheta(t))} & \frac{1}{T_t^i(\vartheta(t))} & 0 & 0 \\ -\frac{1}{R_i(\vartheta(t))T_g^i(\vartheta(t))} & 0 & -\frac{1}{T_g^i(\vartheta(t))} & 0 & 0 \\ \sum_{j=1,j\neq i}^{N} 2\pi T_{ij}(\vartheta(t)) & 0 & 0 & 0 & 0 \\ \beta_i(\vartheta(t)) & 0 & 1 & 0 & 0 \end{bmatrix}.$$

Notice that $A_{ij} = [a_{ls}]_{l,s=1}^5$ with $a_{51} = -2\pi T_{ij}$, and others $a_{ls} = 0$. The parameter $\vartheta(t) \in \mathcal{Q} = \{1, 2, \ldots, Q\}$ is a switching variable. The ACE signal describes the linear combination of the power exchange of the tie line and the frequency deviation, i.e., $ACE_i = \beta_i(\vartheta(t))\Delta f_i(t) + P_{tie}^i(t)$, where ΔP_{tie}^i is the next power exchange of tie line in ith control area. Other parameter meanings are given in Table I.

TABLE I
PHYSICAL MEANING OF PARAMETERS

Parameters	Nomenclature
$\Delta f_i(t)$	i-th frequency deviation
$\Delta P_m^i(t)$	i-th mechanical power output increment
$\Delta Y_i(t)$	i-th valve position
$D_i(\vartheta(t))$	i-th damping coefficient
$T_t^i(\vartheta(t))$	i-th turbine time constant
$T_g^i(\vartheta(t))$	i-th governor time constant
$\beta_i(\vartheta(t))$	i-th frequency bias
$T_{ij}(\vartheta(t))$	coefficient between i-th and j-th area

Accordingly, the ith PI controller is designed as follows:

$$u_i(t) = K_{Pp}^i ACE_i(t) + K_{Ip}^i \int_0^t ACE_i(s)ds = K_p^i y_i(t) \tag{2}$$

where $K_p^i = [K_{Pp}^i \ K_{Ip}^i]$.

To cope with the nonhomogeneity of probabilities, similarly to [35], we introduce a new signal $\{\sigma(t), t \geq 0\}$, which takes values in the set $\mathcal{M} = \{1, 2, \ldots, m\}$. Clearly, for all $t \in [\bar{t}_k^i, \bar{t}_{k+1}^i)$, assuming $\sigma(t) = m$ $(m \in \mathcal{M})$, we define the indicator function

$$\alpha_p^m(t) = \begin{cases} 1, & \vartheta(t) = p, \quad \sigma(t) = m \\ 0, & \text{otherwise} \end{cases} \tag{3}$$

where $\alpha_p^m(t) \geq 0$, $\mathbb{E}\{\sum_{p\in\mathcal{Q}} \alpha_p^m(t)\} = \sum_{p\in\mathcal{Q}} \alpha_p^m = 1$. Thus, the sojourn probability is inferred as follows:

$$\alpha_p^m = \Pr\{\vartheta(t) = p | \sigma(t) = m\}. \tag{4}$$

Remark 1: It is common that the switching process of IMAPS is modeled by an MP in many existing works [36], [37], and the transition probabilities between modes are required to be accessible, which poses difficulties in analyzing switched IMAPS. In contrast, an NSP-based switching model, identified as a key feature, is presented to facilitate the description of random variations of switched IMAPS. As such, the NSPs of finite modes of switched IMAPS are described by a sequence of scalars $\alpha_p^m(t)$. In this way, a novel framework of switched IMAPS is formulated, whose dynamic behavior can be co-revealed by two variables $\vartheta(t)$ and $\sigma(t)$. Compared with the transition probabilities in Markov jump IMAPS, the NSPs are easier to acquire in switched IMAPS.

Remark 2: The DSS $\sigma(t)$, as described in [38], is a critical element in adjusting the feedback information of sojourn probabilities and enables a generalized framework of switched IMAPS for various practical scenarios. For any $\vartheta(t) = p$, the DSS-dependent NSPs are time varying. Benefiting from the ADT strategy, better control performance of switched IMAPS can be expected. Besides, when $\sigma(t) \in \mathcal{M} = \{1\}$, the NSPs degrade to a homogeneous case (i.e., time-invariant sojourn probabilities α_p).

A. Dynamic Quantizer

Apart from the existing logarithmic quantizer, we consider the dynamic quantizer to reduce information exchange frequency and communication load as follows:

$$\text{if } |z| \leq M_1, \text{ then } |q(z) - z| \leq \Delta \tag{5}$$

$$\text{if } |z| \geq M_1, \text{ then } |q(z)| \geq M_1 - \Delta \tag{6}$$

where z is the variable being quantized, Δ stands for the quantization error bound, and M_1 refers to the range of the quantizer. Therefore, the dynamic regulation rules are given by

$$q_{\mu(t)}(z) = \mu(t) q\left(\frac{z}{\mu(t)}\right) \tag{7}$$

where $\mu(t) > 0$ represents the dynamic quantization parameter to be designed.

B. Improved Event-Triggered Protocol

To avoid network congestion, the ETP has been introduced [39] to facilitate the data transmission

$$t_{k+1}^i h = t_k^i h + \min_{l\in\mathbb{N}} \Big\{ lh | e_i^\top(t_k^i h + lh)\Omega_i e_i(t_k^i h + lh) \geq \rho_p y_i^\top(t_k^i h)\Omega_i y_i(t_k^i h) \Big\} \tag{8}$$

where $e_i(t_k^i h + lh) = y_i(t_k^i h + lh) - y_i(t_k^i h)$ stands for the output measurement error, Ω_i is a positive matrix, and $\rho_p \in (0, 1)$ is the threshold coefficient. To further reduce the network congestion effectively, a novel communication strategy, namely, IETP, is presented. Benefiting from the IETP, the following criterion is formulated to judge whether the current packet is released or not:

$$t_{k+1}^i h = t_k^i h + \min_{l\in\mathbb{N}} \Big\{ lh | q_{\mu_1}^\top\big(e_i(t_k^i h + lh)\big)\Omega_{ip} q_{\mu_1}\big(e_i(t_k^i h + lh)\big) \geq \rho_p \mu^\top(t_k^i h + lh)\Omega_{ip}\mu(t_k^i h + lh)\Big)\Big\} \tag{9}$$

where $q_{\mu_1}(e_i(t_k^i h + lh)) = q_{\mu_1}(y_i(t_k^i h + lh)) - q_{\mu_2}(y_i(t_k^i h))$, Ω_{ip} is a mode-dependent positive matrix, $\mu_1 = \mu(t_k^i h + lh)$ and $\mu_2 = \mu(t_k^i h)$. Before further derivation, we divide the interval into the subintervals $[t_k^i h + \eta_k^i, t_{k+1}^i h + \eta_{k+1}^i)$

$$\bigcup_{l=0}^{d} \mathcal{I}_l^i = \left[t_k^i h + \eta_k^i, t_{k+1}^i h + \eta_{k+1}^i\right)$$

where $\mathcal{I}_l^i = [t_k^i h + lh + \eta_{k+l}^i, t_k^i h + lh + h + \eta_{k+l+1}^i]$ and $d = t_{k+1}^i - t_k^i - 1$. In addition, let $\eta(t) = t - t_k^i h - lh$ for $t \in \mathcal{I}_l^i$, which satisfies $0 \leq \eta_k^i \leq \eta_c$. Then, $0 \leq \eta_c \leq \eta(t) \leq h + \eta_c \triangleq \eta_2$.

Remark 3: Added by the ith phasor measurement unit (PMU), the output can be measured in intervals $t_k^i h + lh$. As such, the measured output $y_i(t_k^i h + lh)$ in each control area is transmitted to a dynamic quantizer through a communication link for quantization. In the existing literature concerning the ETPs, the triggering conditions are related to the dynamic states [1], [8], [40]. Differently, to improve resource utilization, an IETP that relates to the dynamic quantization parameter is constructed by determining whether to release the measurement data or not, which renders a distinctive novelty of this study, since more degrees of freedom of the triggering condition can be expected via the presented IETP.

C. Cyber-Attacks

Cyber-attacks can occur in the power grid, which may lead to system instability. Among them, DoS attacks and DAs are two most destructive ones. Let $e_i(t) = q_{\mu_1}(y_i(t_k^i h + lh)) - q_{\mu_2}(y_i(t_k^i h))$, then the actual PI control law is given by

$$u_i(t) = \alpha_i(t)\Big[(1 - \beta_i(t))K_p^i q_{\mu_1}(y_i(t - \eta(t))) - (1 - \beta_i(t)) \times K_p^i e_i(t) + \beta_i(t)K_p^i h\big(q_{\mu_2}\big(y_i\big(t_k^i h\big)\big)\big)\Big] \tag{10}$$

where $\alpha_i(t)$ and $\beta_i(t)$ are two mutually independent Bernoulli random variables, such that $\mathbb{E}\{\alpha_i(t)\} = \bar{\alpha}_i$ and $\mathbb{E}\{\beta_i(t)\} = \bar{\beta}_i$. $q_{\mu_2}(y_i(t_k h))$ denotes the aggression function, which satisfies

$$\left\|h\left(q_{\mu_2}(y_i(t_k h))\right)\right\|_2 \le \left\|H_i q_{\mu_2}(y_i(t_k h))\right\|_2 \tag{11}$$

where H_i is a known matrix.

D. Model Transformation

For the convenience of presentation, we add four columns to matrix B_p^i to make it a full rank matrix in ith area system, that is, $\bar{B}_p^i = [B_p^i \ \hat{B}_p^i]$. Let $\chi_i(t) = (\bar{B}_p^i)^{-1}x_i(t)$. Then, the augmented system is established as follows:

$$\begin{cases} \dot{\chi}(t) = \sum_{p\in\mathcal{Q}} \alpha_p^m(t)\big[\bar{A}_p\chi(t) + \bar{H}_p\Delta P_L(t) + a(t)(1-\beta(t)) \\ \qquad \times \bar{K}_p q_{\mu_1}(y(t-\eta(t))) - a(t)(1-\beta(t))\bar{K}_p e(t) \\ \qquad + a(t)\beta(t)\bar{K}_p h\left(q_{\mu_2}(y(t_k h))\right)\big] \\ y(t) = \sum_{p\in\mathcal{Q}} \alpha_p^m(t)\bar{C}_p\chi(t) \end{cases} \tag{12}$$

where $a(t) = \mathrm{diag}_N\{a_i(t)I\}$, $\beta(t) = \mathrm{diag}_N\{\beta_i(t)I\}$, $h(q_{\mu_2}y(t_k h)) = \mathrm{diag}_N\{h(q_{\mu_2}y_i(t_k^i h))\}$, $\bar{H}_p^i = (\bar{B}_p^i)^{-1}H_p^i$, $\bar{C}_p^i = C_p^i\bar{B}_p^i$, $\bar{A}_p^{ij} = (\bar{B}_p^i)^{-1}A_p^{ij}\bar{B}_p^i$, $\bar{K}_p^i = [K_p^{i\top} \ \ 0]^\top$, $\bar{A}_p = [\bar{A}_p^{ij}]_{j,i=1}^N$, $\bar{B}_p = \mathrm{diag}_N\{\bar{B}_p^i\}$, $\bar{C}_p = \mathrm{diag}_N\{\bar{C}_p^i\}$, $\bar{K}_p = \mathrm{diag}_N\{\bar{K}_p^i\}$, $\bar{H}_p = \mathrm{diag}_N\{\bar{H}_p^i\}$, $\chi(t) = \mathrm{col}1_N\{\chi_i(t)\}$, $y(t) = \mathrm{col}1_N\{y_i(t)\}$, $u(t) = \mathrm{col}1_N\{u_i(t)\}$, and $\Delta P_L(t) = \mathrm{col}1_N\{\Delta P_L^i(t)\}$.

Before proceeding further, the necessary definitions and lemmas are reviewed.

Definition 1 [41]: For a switching signal $\sigma(t)$, if there exist two positive real numbers N_0 and τ_a, such that the number of switches over interval $(t_0, t]$ satisfies $N_\sigma(t_0, t) \le [(t-t_0)/\tau_a] + N_0$, then $\sigma(t)$ is said to have an average residence time τ_a.

Definition 2 [42]: The power system is mean-square exponentially stable (MSES), if for $\Delta P_L(t) = 0$

$$\mathbb{E}\left\{\|\chi(t)\|^2\right\} \le \varepsilon_1 e^{-\varepsilon_2(t-t_0)}\|\chi(t_0)\|_{\mathbb{C}}^2 \tag{13}$$

where $\|\chi(t_0)\|_{\mathbb{C}}^2 = \sup_{-\eta_2\le s\le 0}\{\|\chi(s)\|^2, \|\dot{\chi}(s)\|_{\mathbb{C}}^2\}$.

Definition 3 [8]: For parameters $\gamma > 0$ and $b > 0$, the augmented system (12) is MSES with preset performance, if

$$\int_0^\infty e^{-bs}y^\top(s)y(s)ds < \gamma^2\int_0^\infty \Delta P_L^\top(s)\Delta P_L(s)ds. \tag{14}$$

Lemma 1 [8]: For any symmetric matrices $W > 0$ and $R_1 > 0$, if $\left[\begin{smallmatrix} W & R_1 \\ * & W \end{smallmatrix}\right] \ge 0$, it holds that

$$-\eta_2\int_{t-\eta_2}^t \dot{\chi}^\top(s)W\dot{\chi}(s) \le \varsigma^\top(t)\Xi\varsigma(t)$$

where $\varsigma(t) = \mathrm{col}\{\chi(t), \chi(t-\eta(t)), \chi(t-\eta_2)\}$ and

$$\Xi = \begin{bmatrix} -W & W-R_1 & R_1 \\ * & -2W+He\{R_1\} & W-R_1 \\ * & * & -W \end{bmatrix}.$$

III. Main Results

Theorem 1: The augmented system (12) is MSES, if for some scalars $\eta_2 > 0$, $\gamma > 0$, $b > 0$, $\varsigma > 0$, $\rho_p > 0$, $\kappa > 1$, $\theta > 1$, $M_1 > 0$, matrices $P_p^m > 0$, $M > 0$, $R_1 > 0$, $R > 0$, $W > 0$, $\Omega_p > 0$, Z with compatible dimensions, and any $m, n \in \mathcal{M}$, $p, q \in \mathcal{Q}$, such that

$$P_p^m \le \kappa P_p^n, (m \ne n) \tag{15}$$

the ADT satisfies

$$\tau_a > \tau_a^* = \frac{\ln\kappa}{b} \tag{16}$$

and the following matrix inequalities are valid:

$$\hat{\Xi}_{pm} = \begin{bmatrix} \Xi_{pm}^1 & \Xi_{pm}^2 & \Xi_{pm}^3 \\ * & -\gamma^2 I & 0 \\ * & * & -I \end{bmatrix} < 0 \tag{17}$$

$$\begin{bmatrix} W & R_1 \\ * & W \end{bmatrix} > 0 \tag{18}$$

where

$$\Xi_{pm}^1 = \begin{bmatrix} \Psi_{pm}^1 & \Psi_{pm}^2 \\ * & \Psi_{pm}^3 \end{bmatrix}$$

$$\Xi_{pm}^2 = \begin{bmatrix} \sum\limits_{p\in\mathcal{Q}} \alpha_p^m\bar{H}_p^\top Z & 0 & 0 & \sum\limits_{p\in\mathcal{Q}} \alpha_p^m\bar{H}_p^\top Z & 0 & 0 \end{bmatrix}^\top$$

$$\Xi_{pm}^3 = \begin{bmatrix} \sqrt{\alpha_1^m}\bar{C}_1^\top & \sqrt{\alpha_2^m}\bar{C}_2^\top & \cdots & \sqrt{\alpha_Q^m}\bar{C}_Q^\top \end{bmatrix}$$

$$\Psi_{pm}^1 = \begin{bmatrix} \Upsilon_{pm}^1 & \Upsilon_{pm}^2 & e^{-b\eta_2}R_1 \\ * & \Upsilon_{pm}^3 & e^{-b\eta_2}(W-R_1) \\ * & * & -e^{-b\eta_2}M - e^{-b\eta_2}W \end{bmatrix}$$

$$\Psi_{pm}^2 = \begin{bmatrix} \Upsilon_{pm}^4 & -\sum\limits_{p\in\mathcal{Q}} \alpha_p^m\bar{a}(1-\bar{\beta})Z^\top\bar{K}_p & \sum\limits_{p\in\mathcal{Q}} \alpha_p^m\bar{a}\bar{\beta}Z^\top\bar{K}_p \\ \Upsilon_{pm}^5 & \Upsilon_{pm}^6 & 0 \\ 0 & 0 & 0 \end{bmatrix}$$

$$\Psi_{pm}^3 = \begin{bmatrix} \eta_2^2W - 2\varsigma Z^\top & -\sum\limits_{p\in\mathcal{Q}} \alpha_p^m\varsigma\bar{a}(1-\bar{\beta})Z^\top\bar{K}_p & -\sum\limits_{p\in\mathcal{Q}} \alpha_p^m\varsigma\bar{a}\bar{\beta}Z^\top\bar{K}_p \\ * & -\Omega_p + H^\top H & 0 \\ * & * & -I \end{bmatrix}$$

$$\Upsilon_{pm}^1 = \sum_{p\in\mathcal{Q}} \alpha_p^m P_p^m - e^{-b\eta_2}W + M + \sum_{p\in\mathcal{Q}} \alpha_p^m He\left\{Z^\top\bar{A}_p\right\}$$

$$\Upsilon_{pm}^2 = e^{-b\eta_2}(W-R_1) - \sum_{p\in\mathcal{Q}} \alpha_p^m\bar{a}(1-\bar{\beta})e^{-b\eta_2}R_1 + \sum_{p\in\mathcal{Q}} \alpha_p^m Z^\top\bar{K}_p\left(\frac{\sqrt{\theta}}{M_1}\Delta + I\right)\bar{C}_p$$

$$\Upsilon_{pm}^3 = e^{-b\eta_2}(-2W + He\{R_1\}) + \sum_{p\in\mathcal{Q}} \alpha_p^m\bar{C}_p^\top\left(\frac{\sqrt{\theta}}{M_1}\Delta + I\right) \times H^\top H\left(\frac{\sqrt{\theta}}{M_1}\Delta + I\right)\bar{C}_p$$

$$\Upsilon_{pm}^4 = \sum_{p\in\mathcal{Q}} \alpha_p^m P_p^m - Z^\top + \sum_{p\in\mathcal{Q}} \alpha_p^m\varsigma\bar{A}_p^\top Z$$

$$\Upsilon_{pm}^5 = \sum_{p\in\mathcal{Q}} \alpha_p^m\bar{a}(1-\bar{\beta})\left(\frac{\sqrt{\theta}}{M_1}\Delta + I\right)\varsigma\bar{C}_p^\top\bar{K}^\top Z$$

$$\Upsilon_{pm}^6 = -\sum_{p\in\mathcal{Q}} \alpha_p^m\left(\frac{\sqrt{\theta}}{M_1}\Delta + I\right)\bar{C}_p^\top H^\top H.$$

Proof: Construct the Lyapunov function as below

$$V(\chi(t), \vartheta(t), \sigma(t)) = \sum_{i=1}^3 V_i(\chi(t), \vartheta(t), \sigma(t)) \tag{19}$$

where

$$V_1(\chi(t), \vartheta(t), \sigma(t)) = \chi^\top(t)P_{\vartheta(t)}^{\sigma(t)}\chi(t)$$

$$V_2(\chi(t), \vartheta(t), \sigma(t)) = \int_{t-\eta_2}^t e^{b(s-t)}\chi^\top(s)M\chi(s)ds$$

$$V_2(\chi(t), \vartheta(t), \sigma(t)) = \eta_2\int_{-\eta_2}^0\int_{t+s}^t e^{b(\xi-t)}\dot{\chi}^\top(\xi)W\dot{\chi}(\xi)d\xi ds.$$

First of all, for any $p_1, p_2 \in \mathcal{Q}$, we have

$$\mathbb{E}\left\{\alpha_{p_1}^{\sigma(t)}\alpha_{p_2}^{\sigma(t)}\right\} = \begin{cases} \alpha_{p_1}^{\sigma(t)}, & p_1 = p_2 \\ 0, & p_1 \neq p_2. \end{cases} \tag{20}$$

Let $\mathcal{L}$ be the weak infinitesimal operator, then

$$\mathbb{E}\{\mathcal{L}V_1(\chi(t), p, m)\} = \sum_{p\in\mathcal{Q}} \alpha_p^m He\left\{\dot{\chi}^\top(t) P_p^m \chi(t)\right\} \tag{21}$$

$$\begin{aligned}\mathbb{E}\{\mathcal{L}V_2(\chi(t), p, m)\} &= -bV_2(t) + \chi^\top(t) M\chi(t) - e^{-b\eta_2} \\ &\quad \times \chi^\top(t-\eta_2) M\chi(t-\eta_2)\end{aligned} \tag{22}$$

$$\begin{aligned}\mathbb{E}\{\mathcal{L}V_3(\chi(t), p, m)\} &= -bV_3(t) + \eta_2^2 \dot{\chi}^\top(t) W\dot{\chi}(t) \\ &\quad - \eta_2 \int_{t-\eta_2}^{t} e^{b(s-t)} \dot{\chi}^\top(s) W\dot{\chi}(s) ds.\end{aligned} \tag{23}$$

According to Lemma 1, it follows from (23) that:

$$\begin{aligned}\mathbb{E}\{\mathcal{L}V_3(\chi(t), p, m)\} &= -bV_3(t) + \eta_2^2 \dot{\chi}^\top(t) W\dot{\chi}(t) \\ &\quad + \varsigma^\top(t)\Xi\varsigma(t).\end{aligned} \tag{24}$$

Using the property of the dynamic quantizer (5), one has

$$\begin{aligned} q_{\mu(t)}(y(t)) &= \mu(t) q\left(\frac{y(t)}{\mu(t)}\right) \\ &= \mu(t)\left|q\left(\frac{y(t)}{\mu(t)}\right) - \frac{y(t)}{\mu(t)}\right| + y(t) \\ &\leq \mu(t)\Delta + y(t). \end{aligned} \tag{25}$$

Similarly to [43], the quantization parameter can be assigned as

$$\mu(t) = \frac{\sqrt{\theta}}{M_1}|y(t)| \tag{26}$$

where θ and M_1 are given parameters to achieve better system performance. It is clear that $\theta > 1$ yields the prerequisite $|[y(t)]/[\mu(t)]| < M_1$.

Recalling (12), for any matrix Z, one can get

$$\begin{aligned} 0 = \sum_{p\in\mathcal{Q}} \alpha_p^m(t)\Big[\chi^\top(t)Z^\top + \varsigma\dot{\chi}^\top(t)Z^\top\Big] \\ \times \big[-\dot{\chi}(t) + \bar{A}_p\chi(t) \\ + \bar{H}_p\Delta P_L(t) + a(t)(1-\beta(t))\bar{K}_p q_{\mu_1}(y(t-\eta(t))) \\ - a(t)(1-\beta(t))\bar{K}_p e(t) + a(t)\beta(t)\bar{K}_p h\big(q_{\mu_2}(y(t_k h))\big)\big]. \end{aligned} \tag{27}$$

Furthermore, according to (11), it yields

$$\begin{aligned} h^\top\big(q_{\mu_2}y(t_k h)\big)h\big(q_{\mu_2}y(t_k h)\big) - q_{\mu_2}^\top(y(t_k h)) \\ \times H^\top H q_{\mu_2}(y(t_k h)) \leq 0. \end{aligned} \tag{28}$$

From (19)–(28), it follows that:

$$\mathcal{L}(\chi(t), p, m) \leq -bV(\chi(t), p, m) + \bar{\xi}^\top(t)\Xi_{pm}^1\xi(t) \tag{29}$$

where $\bar{\xi}(t) = [\xi^\top(t)\ \Delta P_L(t)]^\top$, $\xi^\top(t) = [\chi^\top(t), \chi^\top(t-\eta(t)), \chi^\top(t-\eta_2), \dot{\chi}^\top(t), e(t), h^\top(q_{\mu_2}(y(t_k h)))]$. Considering $\Delta P_L(t) = 0$, it implies that $\Xi_{p1}^m < 0$, which yields

$$\mathcal{L}V(\chi(t), p, m) + bV(\chi(t), p, m) \leq 0. \tag{30}$$

Multiplying both sides of (29) by e^t for $t \in [t_{k-1}, t_k)$ yields

$$\begin{aligned} &V(\chi(t), \vartheta(t), \sigma(t)) \\ &\quad \leq e^{-b(t-t_{k-1})} V(\chi(t_{k-1}), \vartheta(t_{k-1}), \sigma(t_{k-1})). \end{aligned} \tag{31}$$

Recalling (15), it renders $P_{\vartheta(t_k)}^{\sigma(t_{k-1})} \leq \kappa P_{\vartheta(t_k)}^{\sigma(t_k)}$. For any $\sigma(t_k), \sigma(t_{k-1}) \in \mathcal{M}$, the following inequality holds:

$$V(\chi(t), \vartheta(t), \sigma(t)) \leq \kappa V\left(\chi\left(t_{k-1}^-\right), \vartheta\left(t_{k-1}^-\right), \sigma\left(t_{k-1}^-\right)\right). \tag{32}$$

Combining (31) and (32) and applying simple iterations, one gets

$$\begin{aligned} &V(\chi(t), \vartheta(t), \sigma(t)) \\ &\leq \kappa e^{-b(t-t_{k-1})} V\left(\chi\left(t_{k-1}^-\right), \vartheta\left(t_{k-1}^-\right), \sigma\left(t_{k-1}^-\right)\right) \\ &\leq \kappa^2 e^{-b(t-t_{k-1})} e^{-b(t_{k-1}-t_{k-2})} V\left(\chi\left(t_{k-2}^-\right), \vartheta\left(t_{k-2}^-\right), \sigma\left(t_{k-2}^-\right)\right) \\ &\leq \cdots \leq \kappa^{N_\sigma(0,t)} e^{-b(t-t_0)} V(\chi(t_0), \vartheta(t_0), \sigma(t_0)) \\ &\leq \kappa^{\left(\frac{t-t_0}{\tau_a}+N_0\right)} e^{-b(t-t_0)} V(\chi(t_0), \vartheta(t_0), \sigma(t_0)) \\ &= \kappa^{N_0} e^{-\left(b-\frac{\ln\mu}{\tau_a}\right)(t-t_0)} V(\chi(t_0), \vartheta(t_0), \sigma(t_0)). \end{aligned} \tag{33}$$

Let $\kappa_1 = \min_{p\in\mathcal{Q}, m\in\mathcal{M}}\{\lambda_{\min}(P_p^m)\}$, then

$$\mathbb{E}\{V(\chi(t), \vartheta(t), \sigma(t))\} \geq \kappa_1\|\chi(t)\|^2. \tag{34}$$

On the other hand, let $\kappa_2 = \max_{p\in\mathcal{Q}, m\in\mathcal{M}}\{\lambda_{\max}(P_p^m)\}$, $\kappa_3 = \lambda_{\max}(M)$, and $\kappa_4 = \lambda_{\max}(W)$, then we can obtain that

$$\begin{aligned} &V(\chi(t_0), \vartheta(t_0), \sigma(t_0)) \\ &\quad \leq \kappa_2\|\chi(t_0)\|^2 + \kappa_3 \int_{t_0-\eta_2}^{t_0} e^{b(s-t_0)}\|\chi(s)\|^2 ds \\ &\quad + \kappa_4 \int_{-\eta-2}^{0}\int_{t_0+s}^{t_0} e^{b(\xi-t_0)}\|\dot{\chi}(\xi)\|^2 d\xi ds \\ &\quad \leq \varepsilon_1\|\chi(t_0)\|_{\mathbb{C}}^2 \end{aligned} \tag{35}$$

where $\varepsilon_1 = (\kappa_2 + [(\kappa_3(1-e^{-b\eta_2}))/b] + [(\kappa_4(b\eta_2 - 1 + e^{-b\eta_2}))/b^2])$, $\|\chi(t_0)\|_{\mathbb{C}}^2 = \sup_{-\eta_2\leq s\leq 0}\{\|\chi(s)\|^2, \|\dot{\chi}(s)\|^2\}$, and $\varepsilon_2 = b - (\ln\mu/\tau_a)$.

According to (33)–(35), we finally obtain

$$\mathbb{E}\left\{\|\chi(t)\|^2\right\} \leq \varepsilon_1\mu^{N_0} e^{-\varepsilon_2(t-t_0)}\|\chi(t_0)\|_{\mathbb{C}}^2. \tag{36}$$

Therefore, according to Definition 2, the augmented system (12) is MSES.

Next, defining $l(t) = y^\top(t)y(t) - \gamma^2\Delta P_L^\top(t)\Delta P_L(t)$, when $\Delta P_L(t) \neq 0$, and taking the Schur complement to (17), one gets

$$\mathbb{E}\{\mathcal{L}V(t) + bV(t) + l(t)\} \leq \bar{\xi}^\top(t)\hat{\Xi}_{pm}\bar{\xi}(t) \leq 0. \tag{37}$$

By using similar iterations and integration of (37) with zero initial condition, we derive

$$\mathbb{E}\{V(t)\} \leq \int_0^s \kappa^{N_\sigma(0,s)} e^{-b(t-s)} l(t) ds. \tag{38}$$

Notice that $V(t) > 0$ and, in view of (17), one has $N_\sigma(0,s)\ln\kappa \leq (s/\tau_a)\ln\kappa < bs$.

Thus, one can conclude that $\int_0^\infty e^{-bs}y^\top(s)y(s)ds < \gamma^2\int_0^\infty \Delta P_L^\top(s)\Delta P_L(s)ds$, which completes the proof. ■

On the basis of MSES in Theorem 1, the controller gains will be carried out in Theorem 2.

Theorem 2: The augmented system (12) is MSES, if for some scalars $\eta_2 > 0$, $\gamma > 0$, $b > 0$, $\varsigma > 0$, $\rho_p > 0$, $\kappa > 1$, $\theta > 1$, $M_1 > 0$, matrices $P_p^m > 0$, $M > 0$, $R_1 > 0$, $R > 0$, $W > 0$, $\Omega_p > 0$, Z with compatible dimensions, and any $m, n \in \mathcal{M}$, $p, q \in \mathcal{Q}$, such that (15) and (16) hold, the following matrix inequality is valid:

$$\hat{\bar{\Xi}}_{pm} = \begin{bmatrix} \bar{\Xi}_{pm}^1 & \Xi_{pm}^2 & \Xi_{pm}^3 & \Xi_{pm}^4 \\ * & -\gamma^2 I & 0 & 0 \\ * & * & -I & 0 \\ * & * & * & -I \end{bmatrix} < 0 \tag{39}$$

where

$$\bar{\Xi}_{pm}^1 = \begin{bmatrix} \bar{\Psi}_{pm}^1 & \bar{\Psi}_{pm}^2 \\ * & \bar{\Psi}_{pm}^3 \end{bmatrix}, \bar{\Psi}_{pm}^1 = \begin{bmatrix} \Upsilon_{pm}^1 & \bar{\Upsilon}_{pm}^2 & e^{-b\eta_2} R_1 \\ * & \bar{\Upsilon}_{pm}^3 & e^{-b\eta_2}(W - R_1) \\ * & * & -e^{-b\eta_2} M - e^{-b\eta_2} W \end{bmatrix}$$

$$\Xi_{pm}^4 = \begin{bmatrix} \sqrt{\alpha_1^m}\bar{C}_1^\top \left(\frac{\sqrt{\theta}}{M_1}\Delta + I\right) H^\top & \sqrt{\alpha_2^m}\bar{C}_2^\top \left(\frac{\sqrt{\theta}}{M_1}\Delta + I\right) H^\top & \cdots \\ \sqrt{\alpha_Q^m}\bar{C}_Q^\top \left(\frac{\sqrt{\theta}}{M_1}\Delta + I\right) H^\top \end{bmatrix}$$

$$\bar{\Psi}_{pm}^2 = \begin{bmatrix} \Upsilon_{pm}^4 & -\sum_{p\in\mathcal{Q}} \alpha_p^m \bar{a}(1-\bar{\beta}) Y\mathcal{K}_p & \sum_{p\in\mathcal{Q}} \alpha_p^m \bar{a}\bar{\beta} Y\mathcal{K}_p \\ \bar{\Upsilon}_{pm}^5 & \Upsilon_{pm}^6 & 0 \\ 0 & 0 & 0 \end{bmatrix}$$

$$\bar{\Psi}_{pm}^3 = \begin{bmatrix} \eta_2^2 W - 2\varsigma Z^\top & -\sum_{p\in\mathcal{Q}} \alpha_p^m \varsigma \bar{a}(1-\bar{\beta}) Y\mathcal{K}_p & -\sum_{p\in\mathcal{Q}} \alpha_p^m \varsigma \bar{a}\bar{\beta} Y\mathcal{K}_p \\ * & -\Omega_p + H^\top H & 0 \\ * & * & -I \end{bmatrix}$$

$$\bar{\Upsilon}_{pm}^2 = e^{-b\eta_2}(W - R_1) - \sum_{p\in\mathcal{Q}} \alpha_p^m \bar{a}(1-\bar{\beta}) e^{-b\eta_2} R_1 + \sum_{p\in\mathcal{Q}} \alpha_p^m Y\mathcal{K}_p \left(\frac{\sqrt{\theta}}{M_1}\Delta + I\right)\bar{C}_p,\ Y = \mathrm{diag}_N\{Y_i\}$$

$$\bar{\Upsilon}_{pm}^3 = e^{-b\eta_2}(-2W + He\{R_1\}),\ Z = \mathrm{diag}_N\{Z_i\}$$

$$\bar{\Upsilon}_{pm}^5 = \sum_{p\in\mathcal{Q}} \alpha_p^m \bar{a}(1-\bar{\beta}) \left(\frac{\sqrt{\theta}}{M_1}\Delta + I\right) \varsigma \bar{C}_p^\top \mathcal{K}_p^\top Y^\top.$$

In addition, the mode-dependent controller gains are given by

$$\bar{K}_p = \left(Z^\top\right)^{-1} Y\mathcal{K}_p.$$

Proof: With the help of the Schur complement, letting $Z^\top \bar{K}_p = Y\mathcal{K}_p$, one obtains (19). In detail, the ith controller gain is given by

$$\bar{K}_p^i = \left(Z_i^\top\right)^{-1} Y_i \mathcal{K}_p^i = \begin{bmatrix} \left(Z_{1i}^\top\right)^{-1} & 0 \\ 0 & \left(Z_{2i}^\top\right)^{-1} \end{bmatrix} \begin{bmatrix} I_p & 0 \\ 0 & 0 \end{bmatrix} \mathcal{K}_p^i.$$

This completes the proof. ∎

IV. Numerical Example

In this section, to show the feasibility of the proposed strategy, a numerical example of the 3-area IMAPS is presented. Suppose that the coefficients are selected as $T_{12}(\vartheta(t)) = 0.2$, $T_{13}(\vartheta(t)) = 0.25$, and $T_{23}(\vartheta(t)) = 0.12$, $\vartheta(t) = 1, 2$. Furthermore, for any $i = 1, 2, 3$, we choose $\mathcal{M} = \mathcal{Q} = \{1, 2\}$, select the sojourn probabilities as $\alpha_1^1 = 0.5$, $\alpha_2^1 = 0.5$, $\alpha_2^1 = 0.8$, $\alpha_2^2 = 0.2$, and set

TABLE II
Parameters of a 3-Area IMAPS

	Mode	$M_i(\vartheta(t))$	$D_i(\vartheta(t))$	$T_t^i(\vartheta(t))$	$T_g^i(\vartheta(t))$	$\beta_i(\vartheta(t))$	$R_i(\vartheta(t))$
Area 1	$r = 1$	10	1.8	0.3	0.12	10	0.05
	$r = 2$	10	1.3	0.35	0.12	10	0.05
Area 2	$r = 1$	12	1.2	0.4	0.12	12	0.05
	$r = 2$	12	1.8	0.4	0.12	12	0.05
Area 3	$r = 1$	12	1.8	0.35	0.12	12	0.05
	$r = 2$	12	1.3	0.35	0.12	11	0.05

$$\hat{B}_p^i = \begin{bmatrix} 0.001 & 0 & 0 & 0 \\ 0 & 0.001 & 0 & 0 \\ 0 & 0 & 0.001 & 0 \\ 0 & 0 & 0.001 & 0.001 \end{bmatrix}.$$

Furthermore, the parameter of DoS attacks is $\bar{a}_i = 0.97$. Set $\gamma = 0.5$, $\eta_2 = 0.0069$, $b = 0.2$, $\kappa = 1.05$, $\theta = 36$, $\Delta = 0.7$, $M_1 = 3$, $\rho_1 = 0.1$, $\rho_2 = 0.5$, and $\varsigma = 0.01$. Additionally, we select $\bar{\beta}_i = 0.06$, and the attack signal is assigned as $h(q_{\mu_2}(y_i(t))) = -\tanh(H_i q_{\mu_2}(y_i(t)))$, where $H_i = \mathrm{diag}\{2, 2\}$. The other nominal parameters are listed in Table II.

According to Theorem 2, the controller gains and the event-triggered weighting matrices with IETP can be calculated as follows:

$$\text{Area 1: } [K_{11}|K_{12}] = [0.3645\ -0.0192|\ -0.0846\ -0.0515]$$
$$[\Omega_{11}|\Omega_{12}] = \begin{bmatrix} 410.6300 & -443.0916 & 48.3322 & -558.2407 \\ -443.0916 & 13439.7314 & -558.2407 & 10304.5419 \end{bmatrix}$$
$$\text{Area 2: } [K_{21}|K_{22}] = [0.3984\ 0.0040\ |\ -0.0175\ -0.0032]$$
$$[\Omega_{21}|\Omega_{22}] = \begin{bmatrix} 1255.9723 & -367.1393 & 96.8227 & -635.3520 \\ -367.1393 & 13614.6861 & -635.3520 & 12569.4672 \end{bmatrix}$$
$$\text{Area 3: } [K_{31}|K_{32}] = [0.3891\ -0.0832\ |\ -0.0606\ 0.0108]$$
$$[\Omega_{31}|\Omega_{32}] = \begin{bmatrix} 1101.8583 & -428.5806 & 36.7036 & -443.6803 \\ -428.5806 & 13417.8197 & -443.6803 & 10582.6098 \end{bmatrix}.$$

Similarly, with the same parameters, the gains and weight matrices of the controller with ETP can be obtained as follows:

$$\text{Area 1: } [K_{11}|K_{12}] = [0.0533\ -0.4668|\ -0.8562\ -0.0023]$$
$$\Omega_1 = \begin{bmatrix} 87.1938 & -357.8390 \\ -357.8390 & 1925.4401 \end{bmatrix}$$
$$\text{Area 2: } [K_{21}|K_{22}] = [0.0313\ 0.0259\ -0.6208\ -0.2583]$$
$$\Omega_2 = \begin{bmatrix} 107.4643 & -467.9744 \\ -467.9744 & 2603.9374 \end{bmatrix}$$
$$\text{Area 3: } [K_{31}|K_{32}] = [0.0259\ 0.0314\ |\ -0.5943\ -0.2570]$$
$$\Omega_3 = \begin{bmatrix} 116.8949 & -517.8551 \\ -517.8551 & 2907.6801 \end{bmatrix}.$$

The initial states are set to $\chi_{10} = [-0.043, -0.06, -0.02, 0.005, 0.4]$, $\chi_{20} = [0.039, -0.08, 0.01, 0.018, 0.07]$,

TABLE III
TRIGGERING NUMBERS FOR DIFFERENT MECHANISMS (SAMPLING: 350 TIMES)

	IETP	ETP
Area 1	11.4000	32.5667
Area 2	21.0667	22.0667
Area 3	23.9000	26.8333

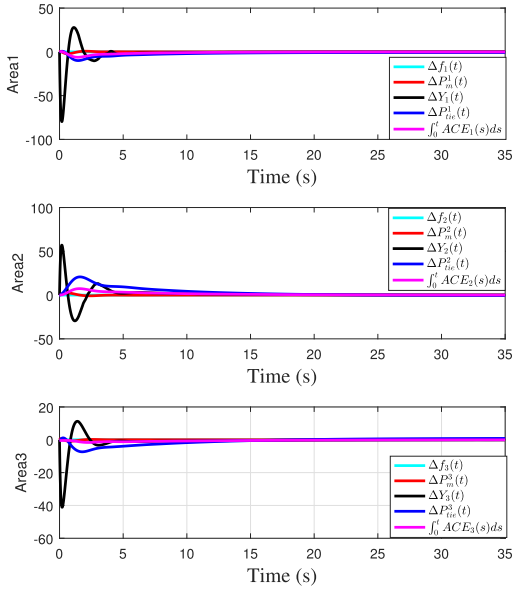

Fig. 2. State $\chi(t)$ of three-area power system with IETP.

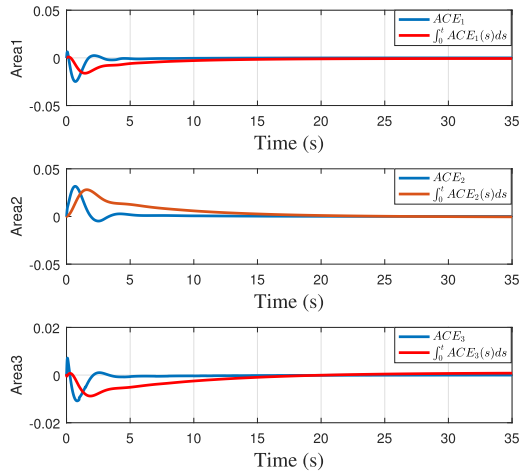

Fig. 3. Output $y(t)$ of three-area power system with IETP.

$\chi_{30} = [-0.0233, -0.002, -0.001, -0.03, -0.46]$, and the disturbance is chosen as follows:

$$\Delta P_L^i(t) = \begin{cases} 0.8\exp(-0.4t)\sin(50t), & t \in [0, 20) \\ 0, & t \in [20, \infty). \end{cases}$$

The simulation results are shown in Figs. 2–7. In the framework of IETP, Figs. 2 and 3 display the state $\chi(t)$ and the measured output $y(t)$ of the 3-area IMAPS. Furthermore, the release intervals and instants with IETP are presented in Fig. 4. These simulation results verify the feasibility of the presented methodology.

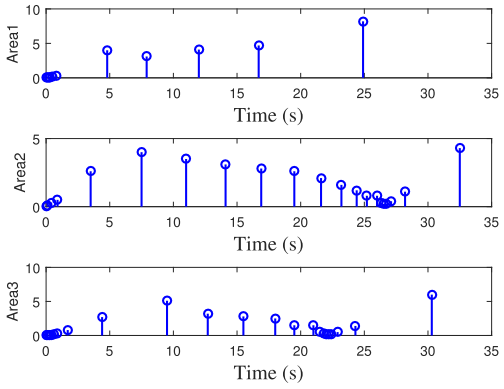

Fig. 4. Release interval and instants with IETP.

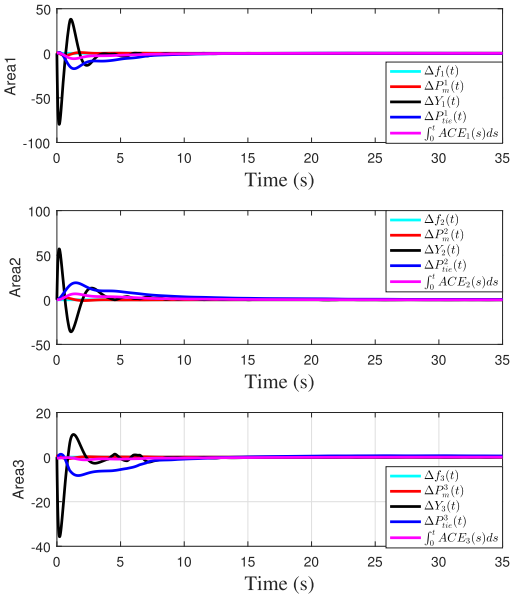

Fig. 5. State $\chi(t)$ of three-area power system with ETP.

To validate the superiority of the proposed IETP, simulation results are compared with those of the conventional ETP as shown in Figs. 5–7. In the framework of traditional ETP, Figs. 5 and 6 display the state $\chi(t)$ and the measured output $y(t)$ of the 3-area IMAPS. Additionally, the release intervals and instants with ETP are presented in Fig. 7. From Figs. 5–7, it is evident that the same control performance can be achieved with fewer packets released when using IETP. These simulation results validate the superiority of the presented methodology.

More specifically, we select the sampling period $h = 0.1$, the triggering numbers for different communication protocols are exhibited in Table III (350 realizations). According to the given data, one can conclude that fewer packets are released using IETP. Thus, in contrast to traditional ETP, the proposed IETP can efficiently alleviate the communication load.

V. CONCLUSION

In this article, an effective quantization-based IETP has been proposed for switched IMAPS under cyber-attacks and NSPs.

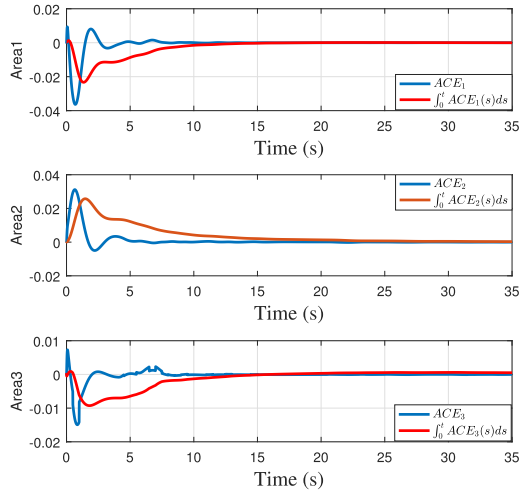

Fig. 6. Output $y(t)$ of three-area power system with ETP.

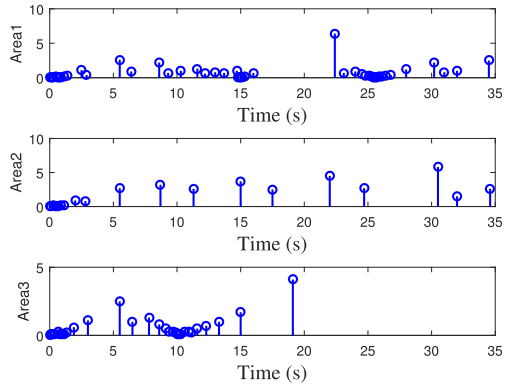

Fig. 7. Release interval and instants with ETP.

To regulate the data transmission with fewer triggering times, an IETP releted to the dynamic quantizer parameter has been presented. By designing NSP-based LFC and IETP, sufficient conditions are derived to ensure that the resulting system is MSES. Finally, simulation results verify the effectiveness of the developed approach. Given the high dimensions and complex structures, extending the derived method to large-scale switching power systems remains our future research direction.

REFERENCES

[1] J. Liu, Y. Gu, L. Zha, Y. Liu, and J. Cao, "Event-triggered $\mathcal{H}_\infty$ load frequency control for multiarea power systems under hybrid cyber attacks," *IEEE Trans. Syst., Man, Cybern., Syst.*, vol. 49, no. 8, pp. 1665–1678, Aug. 2019.

[2] M. Shiroei, M. R. Toulabi, and A. M. Ranjbar, "Robust multivariable predictive based load frequency control considering generation rate constraint," *Int. J. Electr. Power Energy Syst.*, vol. 46, pp. 405–413, Mar. 2013.

[3] C. Peng and J. Zhang, "Delay-distribution-dependent load frequency control of power systems with probabilistic interval delays," *IEEE Trans. Power Syst.*, vol. 31, no. 4, pp. 3309–3317, Jul. 2016.

[4] L. Shanmugam and Y. H. Joo, "Stability and stabilization for T–S fuzzy large-scale interconnected power system with wind farm via sampled-data control," *IEEE Trans. Syst., Man, Cybern., Syst.*, vol. 51, no. 4, pp. 2134–2144, Apr. 2021.

[5] G. Liu, J. H. Park, C. Hua, and Y. Li, "Hybrid dynamic event-triggered load frequency control for power systems with unreliable transmission networks," *IEEE Trans. Cybern.*, vol. 53, no. 2, pp. 806–817, Feb. 2023, doi: 10.1109/TCYB.2022.3163271.

[6] Z. Cheng, S. Hu, D. Yue, C. Dou, and S. Shen, "Resilient distributed coordination control of multiarea power systems under hybrid attacks," *IEEE Trans. Syst., Man, Cybern., Syst.*, vol. 52, no. 1, pp. 7–18, Jan. 2022.

[7] L. Xie, J. Cheng, Y. Zou, Z.-G. Wu, and H. Yan, "A dynamic-memory event-triggered protocol to multiarea power systems with semi-Markov jumping parameter," *IEEE Trans. Cybern.*, early access, Oct. 10, 2022, doi: 10.1109/TCYB.2022.3208363.

[8] A. Kazemy and M. Hajatipour, "Event-triggered load frequency control of Markovian jump interconnected power systems under denial-of-service attacks," *Int. J. Electr. Power Energy Syst.*, vol. 133, Dec. 2021, Art. no. 107250.

[9] J. Cheng, L. Xie, J. H. Park, and H. Yan, "Protocol-based output-feedback control for semi-Markov jump systems," *IEEE Trans. Autom. Control*, vol. 67, no. 8, pp. 4346–4353, Aug. 2022.

[10] W. Qi, G. Zong, Y. Hou, and M. Chadli, "SMC for discrete-time nonlinear semi-Markovian switching systems with partly unknown semi-Markov kernel," *IEEE Trans. Autom. Control*, vol. 68, no. 3, pp. 1855–1861, Mar. 2023.

[11] E. Tian, W. K. Wong, D. Yue, and T.-C. Yang, "$\mathcal{H}_\infty$ filtering for discrete-time switched systems with known sojourn probabilities," *IEEE Trans. Autom. Control*, vol. 60, no. 9, pp. 2446–2451, Sep. 2015.

[12] H. Shen, Z. Huang, J. Cao, and J. H. Park, "Exponential $\mathcal{H}_\infty$ filtering for continuous-time switched neural networks under persistent dwell-time switching regularity," *IEEE Trans. Cybern.*, vol. 50, no. 6, pp. 2440–2449, Jun. 2020.

[13] H. Shen, F. Li, J. Cao, Z.-G. Wu, and G. Lu, "Fuzzy-model-based output feedback reliable control for network-based semi-Markov jump nonlinear systems subject to redundant channels," *IEEE Trans. Cybern.*, vol. 50, no. 11, pp. 4599–4609, Nov. 2020.

[14] T. Li and E. Tian, "Robust $\mathcal{H}_\infty$ control for ICPT process with coil misalignment and time delay: A sojourn-probability-based switching case," *IEEE Trans. Circuits Syst. I, Reg. Papers*, vol. 68, no. 12, pp. 5156–5167, Dec. 2021.

[15] J. Cheng, J. H. Park, X. Zhao, J. Cao, and W. Qi, "Static output feedback control of switched systems with quantization: A nonhomogeneous sojourn probability approach," *Int. J. Robust Nonlinear Control*, vol. 29, no. 17, pp. 5992–6005, 2019.

[16] Z. Cheng, D. Yue, S. Shen, S. Hu, and L. Chen, "Secure frequency control of hybrid power system under DoS attacks via Lie algebra," *IEEE Trans. Inf. Forensics Security*, vol. 17, pp. 1172–1184, 2022.

[17] X. M. Li, Q. Zhou, P. Li, H. Li, and R. Lu, "Event-triggered consensus control for multi-agent systems against false data-injection attacks," *IEEE Trans. Cybern.*, vol. 50, no. 5, pp. 1856–1866, May 2020.

[18] L. Che, X. Liu, Z. Li, and Y. Wen, "False data injection attacks induced sequential outages in power systems," *IEEE Trans. Power Syst.*, vol. 34, no. 2, pp. 1513–1523, Mar. 2019.

[19] P. Chen, J. Li, and M. R. Fei, "Resilient event-triggered $\mathcal{H}_\infty$ load frequency control for networked power systems with energy-limited doS attacks," *IEEE Trans. Power Syst.*, vol. 32, no. 5, pp. 4110–4118, Sep. 2017.

[20] S. Li, Y. Yılmaz, and X. Wang, "Quickest detection of false data injection attack in wide-area smart grids," *IEEE Trans. Smart Grid*, vol. 6, no. 6, pp. 2725–2735, Nov. 2015.

[21] J. Hu, J. Li, Y. Kao, and D. Chen, "Optimal distributed filtering for nonlinear saturated systems with random access protocol and missing measurements: The uncertain probabilities case," *Appl. Math. Comput.*, vol. 418, Apr. 2022, Art. no. 126844.

[22] J. Hu, C. Jia, H. Yu, and H. Liu, "Dynamic event-triggered state estimation for nonlinear coupled output complex networks subject to innovation constraints," *IEEE/CAA J. Automatica Sinica*, vol. 9, no. 5, pp. 941–944, May 2022.

[23] Z. Tang, J. H. Park, Y. Wang, and J. Feng, "Adaptively synchronize the derivative coupled complex networks with proportional delay," *IEEE Trans. Syst., Man, Cybern., Syst.*, vol. 51, no. 8, pp. 4969–4979, Aug. 2021.

[24] D. Wang, D. Wang, and W. Wang, "Necessary and sufficient conditions for containment control of multi-agent systems with time delay," *Automatica*, vol. 103, pp. 418–423, May 2019.

[25] D. Wang, Z. Wang, J. Lian, and W. Wang, "Surplus-based accelerated algorithms for distributed optimization over directed networks," *Automatica*, vol. 146, Dec. 2022, Art. no. 110569.

[26] H. Chen, G. Zong, X. Zhao, F. Gao, and K. Shi, "Secure filter design of fuzzy switched CPSs with mismatched modes and application: A multidomain event-triggered strategy," *IEEE Trans. Ind. Informat.*, early access, Jan. 17, 2023, doi: 10.1109/TII.2022.3232768.

[27] J. Cheng, Y. Wu, H. Yan, Z.-G. Wu, and K. Shi, "Protocol-based filtering for fuzzy Markov affine systems with switching chain," *Automatica*, vol. 141, Jul. 2022, Art. no. 110321.

[28] J. Cheng, L. Xie, D. Zhang, and H. Yan, "Novel event-triggered protocol to sliding mode control for singular semi-Markov jump systems," *Automatica*, vol. 151, May 2023, Art. no. 110906.
[29] G. Guo, L. Ding, and Q.-L. Han, "A distributed event-triggered transmission strategy for sampled-data consensus of multi-agent systems," *Automatica*, vol. 50, no. 5, pp. 1489–1496, 2014.
[30] K. Mohammadi, E. Azizi, J. Choi, M.-T. Hamidi-Beheshti, A. Bidram, and S. Bolouki, "Asynchronous periodic distributed event-triggered voltage and frequency control of microgrids," *IEEE Trans. Power Syst.*, vol. 36, no. 5, pp. 4524–4538, Sep. 2021.
[31] Z. Ye, D. Zhang, Z.-G. Wu, and H. Yan, "A3C-based intelligent event-triggering control of networked nonlinear unmanned marine vehicles subject to hybrid attacks," *IEEE Trans. Intell. Transp. Syst.*, vol. 23, no. 8, pp. 12921–12934, Aug. 2022, doi: 10.1109/TITS.2021.3118648.
[32] H. Shen, D. Wang, Z. Wang, J. H. Park, and K. Shi, "$\mathcal{H}_\infty$ load frequency control for power systems under communication delays: An event-triggered dynamic output feedback scheme," *IEEE Trans. Circuits Syst. II, Exp. Briefs*, vol. 69, no. 8, pp. 3495–3499, Aug. 2022, doi: 10.1109/TCSII.2022.3161009.
[33] Z.-M. Li and J. Xiong, "Event-triggered fuzzy filtering for nonlinear networked systems with dynamic quantization and stochastic cyber attacks," *ISA Trans.*, vol. 121, pp. 53–62, Feb. 2022.
[34] R. Zhao, Z. Zuo, and Y. Wang, "Event-triggered control for networked switched systems with quantization," *IEEE Trans. Syst., Man, Cybern., Syst.*, vol. 52, no. 10, pp. 6120–6128, Oct. 2022, doi: 10.1109/TSMC.2021.3139386.
[35] J. Cheng, L. Liang, J. H. Park, H. Yan, and K. Li, "A dynamic event-triggered approach to state estimation for switched memristive neural networks with nonhomogeneous sojourn probabilities," *IEEE Trans. Circuits Syst. I, Reg. Papers*, vol. 68, no. 12, pp. 4924–4934, Dec. 2021.
[36] V. Ugrinovskii and H. R. Pota, "Decentralized control of power systems via robust control of uncertain Markov jump parameter systems," *Int. J. Control*, vol. 78, no. 9, pp. 662–677, 2005.
[37] S. Kuppusamy, Y. H. Joo, and H. S. Kim, "Asynchronous control for discrete-time hidden Markov jump power systems," *IEEE Trans. Cybern.*, vol. 52, no. 9, pp. 9943–9948, Sep. 2022, doi: 10.1109/TCYB.2021.3062672.
[38] P. Bolzern, P. Colaneri, and G. D. Nicolao, "Markov jump linear systems with switching transition rates: Mean square stability with dwell-time," *Automatica*, vol. 46, no. 6, pp. 1081–1088, 2010.
[39] H. Wang, D. Zhang, and R. Lu, "Event-triggered H_∞ filter design for Markovian jump systems with quantization," *Nonlinear Anal. Hybrid Syst.*, vol. 28, pp. 23–41, May 2018.
[40] P. Chen, D. Zhang, L. Yu, and H. Yan, "Dynamic event-triggered output feedback control for load frequency control in power systems with multiple cyber attacks," *IEEE Trans. Syst., Man, Cybern., Syst.*, vol. 52, no. 10, pp. 6246–6258, Oct. 2022, doi: 10.1109/TSMC.2022.3143903.
[41] J. P. Hespanha, "Uniform stability of switched linear systems: Extensions of LaSalle's invariance principle," *IEEE Trans. Autom. Control*, vol. 49, no. 4, pp. 470–482, Apr. 2004.
[42] K. Ding and Q. Zhu, "Extended dissipative anti-disturbance control for delayed switched singular semi-Markovian jump systems with multi-disturbance via disturbance observer," *Automatica*, vol. 128, no. 6, 2021, Art. no. 109556.
[43] X.-H. Chang, Z.-M. Li, and J. H. Park, "Fuzzy generalized $\mathcal{H}_2$ filtering for nonlinear discrete-time systems with measurement quantization," *IEEE Trans. Syst., Man, Cybern., Syst.*, vol. 48, no. 12, pp. 2419–2430, Dec. 2018.

Jun Cheng received the B.S. degree in mathematics and applied mathematics from the Hubei University for Nationalities, Hubei, China, in 2010, and the Ph.D. degree from the University of Electronic Science and Technology of China, Chengdu, China, in 2015.

From 2015 to 2019, he is a Staff with the Hubei University for Nationalities. He was a Visiting Scholar with the Department of Electrical and Computer Engineering, National University of Singapore, Singapore, from 2013 to 2014, and the Department of Electrical Engineering, Yeungnam University, Gyeongsan, South Korea, in 2016 and 2018. Since 2019, he has been with Guangxi Normal University, Guilin, China, where he is currently a Professor with the School of Mathematics and Statistics. His current research interests include analysis and synthesis for stochastic hybrid systems, networked control systems, robust control, and nonlinear systems.

Dr. Cheng has been a recipient of the Highly Cited Researcher Award listed by Clarivate Analytics since 2019. He serves as an Associate Editor for several international journals, including *Journal of The Franklin Institute* and *International Journal of Control, Automation, and Systems*.

Jiangming Xu received the B.S. degree in mathematics and applied mathematics from Lingnan Normal University, Zhangjiang, China, in 2021. She is currently pursuing the master's degree in applied mathematics with Guangxi Normal University, Guilin, China.

Her current research interests include semi-Markov jump systems, singular perturbation systems, power systems, event-triggered control, and sliding-mode control.

Ju H. Park (Senior Member, IEEE) received the Ph.D. degree in electronics and electrical engineering from the Pohang University of Science and Technology (POSTECH), Pohang, Republic of Korea, in 1997.

From May 1997 to February 2000, he was a Research Associate with the Engineering Research Center-Automation Research Center, POSTECH. He joined Yeungnam University, Kyongsan, Republic of Korea, in March 2000, where he is currently the Chuma Chair Professor. He has coauthored the monographs *Recent Advances in Control and Filtering of Dynamic Systems with Constrained Signals* (New York, NY, USA: Springer–Nature, 2018) and *Dynamic Systems With Time Delays: Stability and Control* (New York, NY, USA: Springer–Nature, 2019), and is an Editor of an Edited Volume *Recent Advances in Control Problems of Dynamical Systems and Networks* (New York: Springer–Nature, 2020). His research interests include control theories, neural/complex networks, fuzzy systems, and intelligent vehicles. He has published a number of articles in these areas.

Dr. Park has been a recipient of the Highly Cited Researchers Award by Clarivate Analytics (formerly, Thomson Reuters) since 2015, and listed in three fields, Engineering, Computer Sciences, and Mathematics, from 2019 to 2022. He is a Subject Editor/Advisory Editor/Associate Editor/Editorial Board Member of several international journals, including *Nonlinear Dynamics*, *IET Control Theory & Applications*, *Applied Mathematics and Computation*, *The Journal of The Franklin Institute*, *Engineering Reports*, *Cogent Engineering*, *Franklin Open*, the IEEE TRANSACTIONS ON FUZZY SYSTEMS, the IEEE TRANSACTIONS ON NEURAL NETWORKS AND LEARNING SYSTEMS, and the IEEE TRANSACTIONS ON CYBERNETICS. He is a Fellow of the Korean Academy of Science and Technology.

Michael V. Basin (Senior Member, IEEE) received the Ph.D. degree in physical and mathematical sciences with major in automatic control and system analysis from the Moscow Aviation University, Moscow, Russia, in 1992.

He is currently a Full Professor with the Autonomous University of Nuevo Leon, San Nicolas de los Garza, Mexico, and the Ningbo University of Technology, Zhejiang, China. Starting from 1992, he published more than 400 research papers in international referred journals and conference proceedings. He has supervised 17 doctoral and ten master's theses. He has authored the monograph "New Trends in Optimal Filtering and Control for Polynomial and Time-Delay Systems," (Springer). His works are cited more than 7000 times (H-index = 47). His research interests include optimal filtering and control problems, stochastic systems, time-delay systems, identification, sliding-mode control and variable structure systems, and applications to mechatronic and transportation systems.

Dr. Basin was awarded a title of Highly Cited Researcher by Thomson Reuters, the publisher of Science Citation Index, in 2009 and listed in "100 000 Leading Scientists in the World"; he is a regular member of the Mexican Academy of Sciences and a recipient of the Kimura Best Paper Award from Asian Control Association. He has served as the Editor-in-Chief and serves as the Co-Editor-in-Chief of *The Journal of the Franklin Institute*, the Senior Editor of IEEE/ASME TRANSACTIONS ON MECHATRONICS, an Associate Editor of *Automatica*, *IEEE Transactions on Systems, Man, and Cybernetics: Systems*, *IET-Control Theory & Applications*, *International Journal of Systems Science*, and *Neural Networks*. He has been honored as a Fellow of Prominent Talent (Qian Ren) Program of Zhejiang Province, China.